A COMPUTATIONAL STUDY
OF THE FRACTURE BEHAVIOUR OF CONCRETE IN A
MODIFIED SPLIT HOPKINSON BAR TEST

R. R. Pedersen[1], L. J. Sluys[1], J. Weerheijm[1,2] and A. Simone[3]

[1]Faculty of Civil Engineering and Geosciences, Delft University of Technology P.O. Box 5048, 2600 GA Delft, The Netherlands
[2]TNO Prins Maurits Laboratorium P.O. Box 6050, 2600 JA Delft, The Netherlands
[3]Department of Applied Physics, University of Groningen, 9747 AG Groningen, The Netherlands

ABSTRACT

For a numerical prediction of the response of concrete structures under extreme dynamic loading, reliable material data and material models are crucial. A modified Split Hopkinson Bar, SHB, test methodology is used to determine the material properties in tension at high loading rates which are used in numerical models simulating progressive fracturing. The main focus of this paper is to examine the predictive capability of existing classical and regularised continuum models in reproducing the SHB experiments. These models are based on continuum damage theories in which the net effect of fracture is idealised as a degradation of elasticity of the material. Strain-rate dependency of materials subjected to an impulsive loading is taken into account by including viscous terms in the continuum description. The examples here give an indication of the sensitivity of the model parameters in the computational models and the coupled viscoplastic damage model shows the promising capability of simulating the fracture process of the SHB test. The effect and physical interpretation of the parameters and their mutual dependency in dynamics are not sufficiently understood, and more work is needed to present a physically realistic model for concrete under high loading rates based on micro-mechanics to account for the true mechanisms that cause the strength increase.

1 INTRODUCTION

Concrete is a highly rate-dependent material at loading rates exceeding 15 GPa/s. This means that the apparent macroscopic mechanical properties of concrete depend on the applied loading rate, particularly the material strength but also, to a smaller extent, the Young's modulus and the fracture energy. For the predictive capabilities of computational methods this rate effect should be properly taken into account. Phenomenological rate-dependent models for concrete loaded in tension have been developed in the past. However they lack a physical background. A new category of models should be developed in which rate-dependency is properly taken into account where the micro/meso-structure of the material plays an important role. Part of the strengthening effect is caused by the change of failure mechanisms at micro/meso-level at higher loading rates and by the effect of micro/meso-inertia. For identification of the rate-dependent material properties, a com-
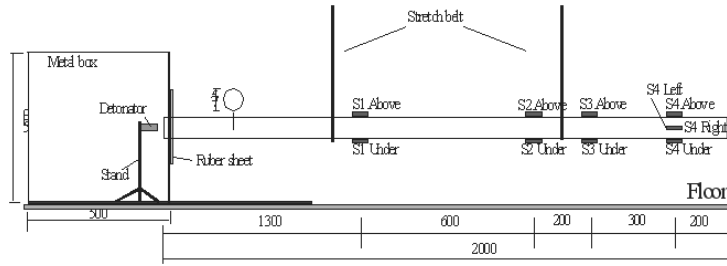
Figure 1: Modified Split Hopkinson Bar test set-up: the concrete specimen (not shown here) is placed at the right end of the steel bar and S1-S4 represent locations of the strain gauges (dimensions in mm).

bined experimental/computational strategy is essential in order to derive an objective set of material parameters. In the experimental part of the work a modified Split Hopkinson Bar test is used, with loading rates up to 1000 GPa/s. From these tests the dynamic material properties are determined. However, several uncertainties are still present and many questions come out of the experiments, and in the future an improved test series will be performed. The computational part of the work is used to improve the experiments which again will be used in the development of the advanced computational models. The first performed SHB test from 2003 [4] is simulated using phenomenological numerical models in order to predict the global and local response and observe the mechanical behaviour of stress waves propagating in the specimen. A pure damage continuum description and a coupled damage viscoplastic approach [2] are utilised. In the next section the set-up and results from the modified SHB tests are briefly described while some results related to the computational part are presented in Section 3.

2   MODIFIED SPLIT HOPKINSON BAR TEST

A modified Split Hopkinson Bar test methodology is utilised. The test set-up is depicted Figure 1. The blast is applied at the left-hand side of a 2000 mm steel bar and the 240 mm notched concrete specimen is placed at the right-hand side of the steel bar. The incident compression wave in the steel bar is transmitted to the specimen and, after reflection at the free end, tensile waves cause failure of the concrete specimen in the notch area. Figure 2 shows the applied load pulse with a duration T of $7.0 \cdot 10^{-5}$ s. The same load pulse is used in the numerical simulations.

The SHB technique combined with sophisticated instrumentation have been used to quantify the dynamic properties of concrete at loading rates of 1000 GPa/s for which hardly any data was available. From the first test series the only data available are the measurements of strains in the concrete specimen. The dynamic properties for concrete derived from the experiments are listed in the table reported in Figure 3. The wave velocity is determined by the transmission time between eight defined locations of the strain gauges. From the velocity the dynamic Young's modulus can be derived using the material density. The tensile strength is determined from the strain measurements beyond the failure zone and the dynamic Young's modulus. Inertia effects will increase the strength of the material due to a time delay in the failure process. Stress concentrations at the notches imply
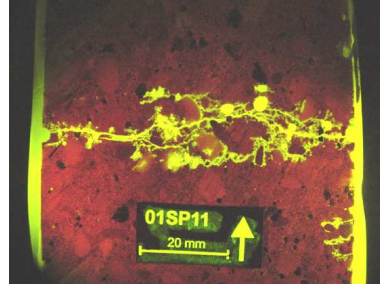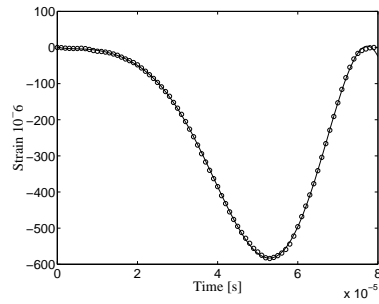
Figure 2: Left: The measured load pulse from the experiments used in the numerical simulations ($7.0 \cdot 10^{-5}$ s). Right: Crack pattern in a specimen with a 2 mm notch (the width of fracture zone is about 20 mm).

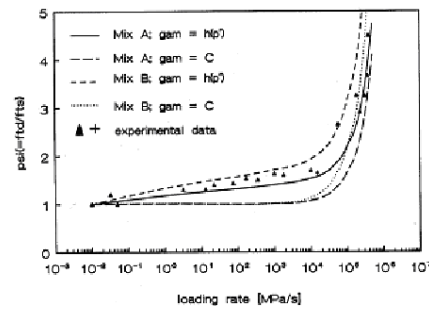|		Static	Dynamic
Young's modulus, E	[GPa]	37.0	46.2
Density, ρ	$\left[\frac{kg}{m^3}\right]$	2400	2400
Poisson ratio, ν		0.2	0.2
Compressive Strength, f_c	[MPa]	40	40
Tensile Strength, f_t	[MPa]	3	15.9
Fracture Energy, G_f	$\left[\frac{J}{m^2}\right]$	100	$230 - 300$

Figure 3: Static and dynamic material properties (loading rate is set to 1000 GPa/s [4]; rate effect of the compression strength is not measured.)

Figure 4: Rate effect on tensile strength for different concrete mixtures [3].

an early crack initiation and therefore the measured tensile strength is lower than the real material strength. These effects are examined in more detail in the following computational models. A factor 5.3 between the static and dynamic tensile strength is determined from the tests which corresponds to data from the literature, see Figure 4. A thorough discussion of the results is given in [4].

3 COMPUTATIONAL MODELLING OF FRACTURE

The finite-element model of the test set-up reported in Figure 1 is shown in Figure 5. The load pulse is applied directly to the concrete specimen (hatch) at $x = 480$ mm where the nonlinear models are used. This implies a compression pulse in the test specimen and a tension wave in the other part of the beam where the concrete material is linear elastic. The length of the beam is chosen such that the tensile waves will not reflect and interfere with the wave in the concrete specimen. The cylindrical geometry of the specimen is approximated by a two-dimensional FE model. In the numerical simulation of the SHB tests a local damage model, LD, and a viscoplastic model coupled to damage, VPD, are considered. An implicit Newmark scheme is utilised with $\beta = 0.25$ and $\gamma = 0.50$ and with time steps of $\Delta t = 5.0 \cdot 10^{-7}$ s and $\Delta t = 2.5 \cdot 10^{-7}$ s for the coarse and fine mesh,
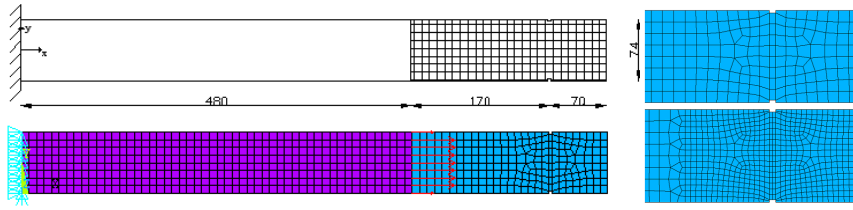
Figure 5: Left: A cantilever beam model of the SHB test set-up (dimensions in mm). Right: The two utilised discretisations using Q4 elements (the front of the compression wave reaches the free end at $t = 5.54 \cdot 10^{-5}$ s and the reflected wave hits the notch at $t = 7.07 \cdot 10^{-5}$ s; the wave velocity and the wave length are $c = 4.39 \cdot 10^6$ mm/s and $\lambda = 300$ mm, respectively). The hatch area is the concrete specimen.

	LD	VPD 1	VPD 2
Softening curve, b		25000	25000
Softening curve, a		1	1
Damage law, α	1	1	1
Damage law, β	1000	8000	30000
Relaxation time, τ		1 s	12 s
Tensile strength, f_t	15.9 MPa	15 MPa	11 MPa

Figure 6: Parameters for the computations (see [2] for an explanation of the symbols).
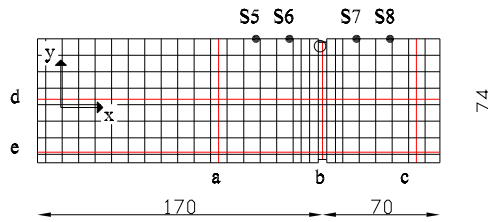

Figure 7: Reference locations for the results depicted in Figure 8: $S5$ ($x = 610$ mm), line d ($y = 38$ mm) and integration point (circle) close to the notch (distances are measured with reference to Figure 5).

respectively. An exponential softening law is used with the model parameters shown in Figure 6 for the isotropic local damage model. From the measurement at the surface of the specimen no damage or nonlinear effects were observed due to the compression pulse. That is why an isotropic damage model is used with Mazars model for the equivalent strain, e.g. only positive strains are considered. In [1] it is shown that, due to the Poisson's effect, positive lateral strains cause damage initiation in the compression phase for low threshold values. To avoid this effect, the dynamic tensile strength of 15.9 MPa is used. The results obtained with the local damage model are strongly mesh dependent as shown in Figures 8 and 9, where the equivalent strain localises in one row of elements close to the notch. Better results can be obtained by using a rate-dependent elastoplastic-damage model. In this model, rate-dependency is considered in the framework of Perzyna viscoplasticity with the Rankine yield criterion expressed in the effective stress space [2]. Because of the regularisation it is possible to obtain mesh independent results and a localisation zone of a certain width. Here, two different examples are presented, VPD 1 and VPD 2 (with model parameters reported in Figure 6). Objective results are obtained with the two element discretisations (see Figure 8). From VPD 1 it is clear that a low viscosity and high tensile strength result in a more brittle material behaviour and a narrow width of the failure zone. The spreading of the failure zone in VPD 2 is higher due to a higher relaxation time but also because of a lower tensile strength. High values for β result in a steep softening curve
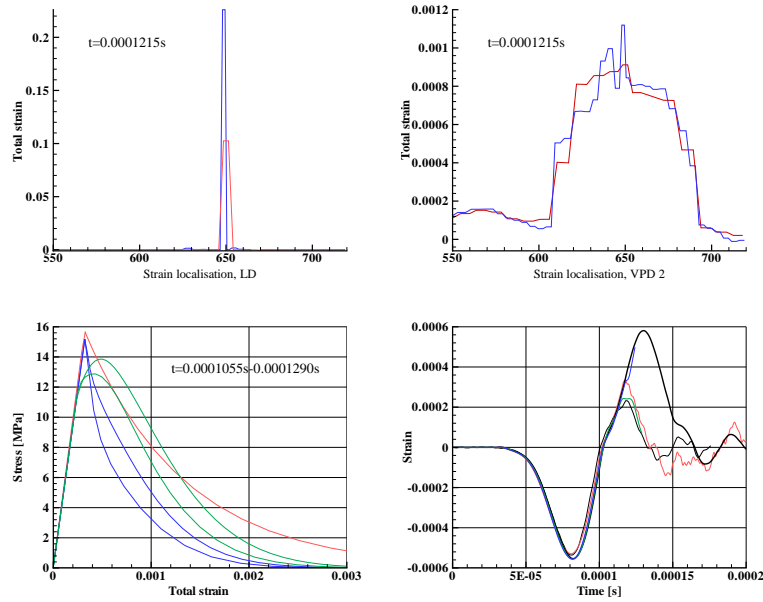
Figure 8: The top pictures show the regularisation effect of the viscoplastic damage model, VPD 2 (right), compared to the response of the local damage model, LD (left), at $t = 0.1215 \cdot 10^{-3}$ s (fine mesh in blue versus coarse mesh in red). Depicted in the bottom-left picture are the stress-strain curves for the integration point close to the notch. These curves show a dependence on the mesh size (red line = LD, blue lines = VPD 1, green lines = VPD 2, top lines = fine mesh; the compression phase is not plotted). The strain-time curves at the integration point close to S5 (bottom-right picture) show that the response from VDP 2 (green) comes close to the measurement of the SHB test (thin black line) while VDP 1 (blue) follows the elastic solution for a longer time (bold black line); the red curve is the response of the local damage model.

but also in a narrow localisation zone. It is shown that a higher value for β is necessary in the damage model coupled to viscosity in order to obtain a comparable softening curve as obtained with the local damage model. For the brittle material behaviour a straight crack forms between the notches while in case of a higher viscosity there is a tendency to form a v-shaped crack.

4   CONCLUSIONS

It is difficult to determine a set of model parameters such that the failure zone in the modified SHB test is comparable to the one from the experiment. However, the response from VPD 2 comes close to the strain measurement and also the width of the fracture zone is not far from the crack pattern observed in the tests. In the local damage model the dynamic tensile strength is explicitly defined but in the viscoplastic damage model the increasing strength is defined implicitly through the viscosity. Consequently, it is unrealistic to use the static tensile strength in the viscoplastic damage model and transmit the strengthening effect to the viscosity alone.
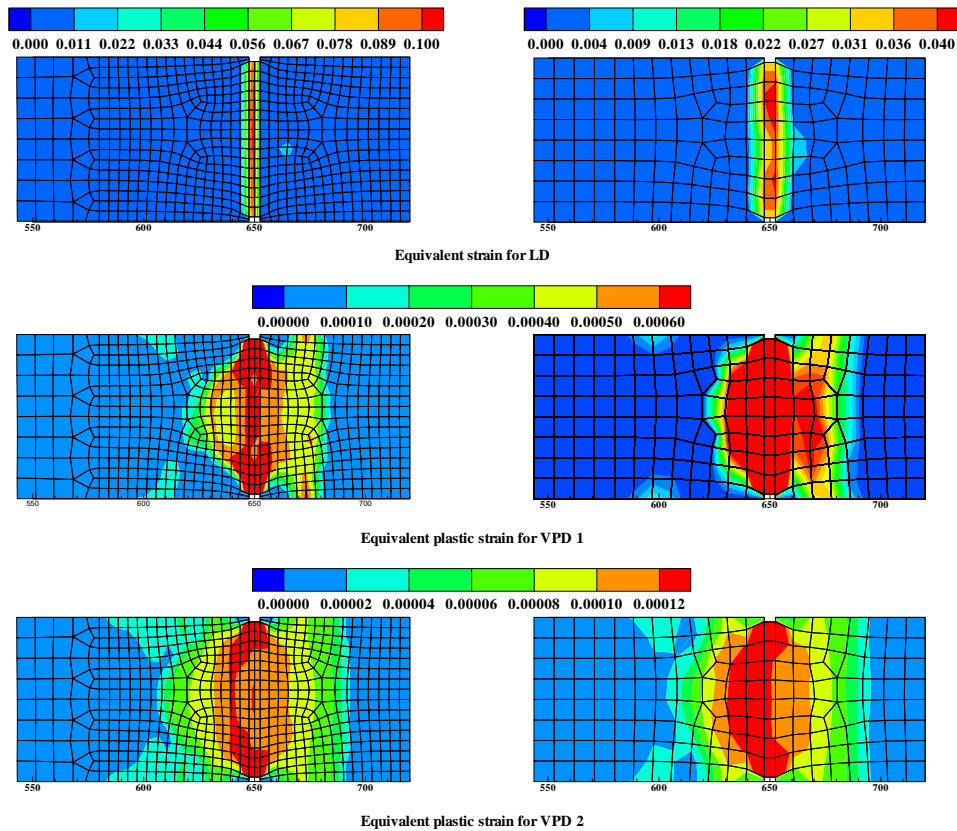
Figure 9: From the local damage model the main crack will run in a straight line between the two notches, as illustrated by the equivalent strain in the figures at the top. Due to the viscous effect, the viscoplastic damage model is able to predict a certain area for micro cracking as can be seen from the plots of the equivalent plastic strain at the bottom. Because of the high viscosity, VPD 2 shows a higher spreading of the failure zone (results reported at $t = 0.1215 \cdot 10^{-3}$ s).

REFERENCES

[1] R. R. Pedersen. A computational study of the fracture behaviour of concrete in a shb test. Technical report, Delft University of Technology, Delft, the Netherlands, 2004.

[2] A. Simone and L. J. Sluys. The use of displacement discontinuities in a rate-dependent medium. *Computer Methods in Applied Mechanics and Engineering*, 193:3015–3033, 2004.

[3] J. Weerheijm. *Concrete under Impact Tensile Loading and Lateral Compression*. PhD thesis, Delft University of Technology, 1992.

[4] J. Weerheijm, J.C.A.M van Doormaal, and R.M. van de Kasteele. Development of a new test set-up for dynamic tensile tests on concrete under high loading rates. Technical Report PML 2003-A87, TNO Prins Maurits Laboratory, Delft, the Netherlands, 2003.